



Contents lists available at ScienceDirect

Nuclear Instruments and Methods in Physics Research B

journal homepage: www.elsevier.com/locate/nimb

The role of the wave packet coherence on the ionization cross section of He by p^+ and C^{6+} projectiles

F. Navarrete^{a,*}, M.F. Ciappina^{b,c}, L. Sarkadi^d, R.O. Barrachina^a

^a Centro Atómico Bariloche e Instituto Balseiro (Comisión Nacional de Energía Atómica and Univ. Nac. de Cuyo), Bariloche, Río Negro, Argentina

^b Max-Planck-Institut für Quantenoptik, Hans-Kopfermann-Strasse 1, D85748 Garching, Germany

^c Institute of Physics of the ASCR, ELI-Beamlines Project, Na Slovance 2, 182 21 Prague, Czech Republic

^d Institute for Nuclear Research of the Hungarian Academy of Sciences (MTA Atomki), P.O. Box 51, H-4001 Debrecen, Hungary

ARTICLE INFO

Article history:

Received 18 November 2016
Received in revised form 30 April 2017
Accepted 17 May 2017
Available online xxx

Keywords:

Coherence
Atomic
Collisions
Ions

ABSTRACT

We study the role of the projectile coherence in collision processes. We analyze in particular the ionization of He by p^+ and C^{6+} projectiles at 1 and 100 MeV/amu, respectively. We compare the influence of this effect in both cases by performing a *First Born* calculation convoluted with a gaussian distribution, which accounts for the initial incoherence of the projectile wave packet. Even though this is the simplest approach that one could implement to solve this problem, it gives good agreement with the experimental results.

© 2017 Elsevier B.V. All rights reserved.

1. Introduction

In the last few years there has been an increasing interest on the projectile coherence effects in ion-atom and ion-molecule collisions [1–10]. In the traditional way to compute the (multiply) differential cross section [11] of a reaction, the projectile wave packet is considered as a plane-wave, though a more realistic model has proved to be necessary to account for the discrepancies found between theory and experiment in some remarkable cases [12].

The degree of transverse coherence of a projectile beam is given by the *coherence length* Δr which is a spatial quantity for which we will give an expression in the next section.

2. Gaussian projectile wave packet

We will consider that, in our collision problem, we have a projectile beam of momentum K_i at the beginning of the reaction, described by minimal gaussian wave packets of width Δx_0 passing through a collimator. The degree of coherence Δr when it reaches the target is given by the following equation [13,14] (Atomic units are used throughout this article):

$$\Delta r = \sqrt{(\Delta x_0)^2 + \frac{(\gamma L/K_i)^2}{(\Delta x_0)^2 + D^2}}, \quad (1)$$

where L is the distance from the target to the collimator, D is the characteristic length of the collimator (as, for instance, the diameter of a circular collimator), and γ is a dimensionless parameter which depends on the shape of the incoherent distribution, and on how its width is defined [14]. The degree of coherence of a wave front is related to the maximum distance at which two points can interfere. For a plane wave, the coherence length is infinitely large because every two points of the wave front interfere, *i.e.* it is completely coherent. A wave front for which the coherence length is small when compared to the size of the target is said to be incoherent.

2.1. Fraunhofer limit

For large values of L , which is the case in a typical collision experiment, we can approximate Eq. (1) by:

$$\Delta r = \frac{\gamma L/K_i}{\sqrt{(\Delta x_0)^2 + D^2}}. \quad (2)$$

In principle, the value of Δx_0 is difficult to estimate, but we can assume that it is small compared to D which is macroscopical. Because of this, we can further simplify the last equation by:

* Corresponding author.

E-mail address: navarrete@cab.cnea.gov.ar (F. Navarrete).

$$\Delta r = \frac{\gamma L}{K_i D}, \quad (3)$$

which is similar to the expression usually found in studies that include coherence effects in the calculation of the cross sections [4,15]. It is important to point out that the degree of coherence must not be confused with the quality of the collimation. While the collimation is more a semi-classical estimation which treats projectiles as a flux of classical point particles, the degree of coherence is inherent to the wave function nature of the projectile and therefore it cannot be suppressed. Both are given by the macroscopic parameters of the experiment, but are qualitatively different.

3. Calculation of the cross section for a gaussian wave packet projectile

In earlier theoretical calculations, the differential cross section for single ionization: $d\sigma/d\mathbf{k}d\mathbf{K}d\mathbf{K}_R$ where $\mathbf{k}, \mathbf{K}_i, \mathbf{K}$ are the momenta of the electron, the ionized target, and the projectile, respectively, is usually derived by describing the incident projectile as a plane wave, which in our framework means a fully coherent wave front.

Karlovets et al. [15] studied the scattering of wave packets off a potential field, with their mean momentum strongly centered at a given value. They arrived to a simple general expression for the differential cross section, similar to that also used previously by other authors [16–19] studying related topics. The differential cross section for an incoming wave packet of general form strongly centered in the initial mean momentum \mathbf{K}_i reads,

$$\frac{d\sigma}{d\mathbf{k}d\mathbf{Q}d\mathbf{K}_R} = \int d\mathbf{Q}'_{\perp} \frac{d\sigma}{d\mathbf{k}d\mathbf{Q}'_{\perp}d\mathbf{K}_R} |\Phi_{\perp}(\mathbf{Q}'_{\perp} - \mathbf{Q}_{\perp})|^2. \quad (4)$$

Here we have written the cross section in terms of the momentum transfer $\mathbf{Q} = \mathbf{K}_i - \mathbf{K}$. In our case, we will take the wave packet in the perpendicular direction, $\Phi_{\perp}(\mathbf{Q}'_{\perp} - \mathbf{Q}_{\perp})$, with a gaussian shape:

$$\Phi_{\perp}(\mathbf{Q}'_{\perp} - \mathbf{Q}_{\perp}) = \frac{1}{\sqrt{2\pi\sigma_x\sigma_y}} \exp\left(-\frac{(Q'_x - Q_x)^2}{4\sigma_x^2} - \frac{(Q'_y - Q_y)^2}{4\sigma_y^2}\right), \quad (5)$$

where x and y are mutually perpendicular axes (x lies in the scattering plane). Both are, in turn, perpendicular to z , the initial direction of the projectile. σ_x and σ_y are the dispersion coefficients of the gaussian. Smaller values of σ_x and σ_y means a narrower gaussian, and thus, a more coherent wave. In fact, by the Heisenberg uncertainty principle, we expect that

$$\sigma_x \propto \frac{1}{\Delta r_x}, \quad (6)$$

and an equivalent expression for σ_y .

For the calculation of the fully differential cross section (FDSC) and the doubly differential cross section (DDCS) we will use a *First Born* approximation, which has proved to be useful for the type of convolution that we are performing [16,19,20].

4. Results

In this section we show the results calculated both coherently and incoherently, and compare them with experimental data [12,21]. In both of the two experiments that we are considering, He was used as a target. We model it as a hydrogen-like atom, so as to deal with a three body problem.

The cross sections are shown as a function of the azimuthal and polar angle of the final electron momentum, ϕ_e and θ_e , respectively. The azimuthal angle is measured from the direction of the x com-

ponent of the momentum transfer $\mathbf{Q} = (Q_x, Q_y, Q_z)$, which is written in cartesian coordinates.

For the incoherent calculation of the cross sections, we will determine the values for the parameters σ_x and σ_y , by fitting Eq. (4) to the measured cross sections.

4.1. C^{6+} at 100 MeV/amu on He

The first set of data that we analyze comes from the work of Schulz et al. [12]. They used C^{6+} projectiles at 100 MeV/amu. The final energy of the electron is fixed at $E_e = 6.5$ eV, and the momentum transfer is evaluated at $Q_x = 0.75$ au and $Q_y = 0.02$ au. By fitting Eq. (4) with the experimental data, we found the values: $\sigma_x = 0.25$ au and $\sigma_y = 0.5$ au. The corresponding coherence lengths are smaller than the Bohr radius of He, thus the wave packet nature of the projectile is expected to have a noticeable effect on the incoherent calculation of the FDSC. In Fig. 1 we can see a good agreement in the scattering plane ($\phi_e = 0$) between the theoretical calculations and the experimental data.

In Fig. 2 we see that for the perpendicular plane ($\phi_e = \pi/2$), the theoretical result of the FDSC calculated in the traditional way gives no satisfactory results neither qualitatively nor quantitatively, while the curve given by Eq. (4) provides a good agreement with the experimental data.

Although in the experimental work of 2003 [12], the coherence length was not taken into account, in a later work [3], it was estimated to be about $\Delta r = 0.001$ au. This is a very small coherence length (even smaller than our estimation), which means that the collision is highly incoherent and a simplified model like the one we are using in this approach would lead to a great blurring of the FDSC, as explained in [10]. Therefore, a more rigorous treatment of the degree of coherence of the projectile wave packet in the calculation of the FDSC would be necessary in this case.

We can point out that because of the inverse dependence of the coherence length on the initial momentum K_i , which in our case is of the order of 1.3×10^6 au, even if the experiment with C^{6+} was performed in an experimental setup with a storage ring [3] which provides a more coherent result, the coherence length would still be smaller than the Bohr radius of the He target.

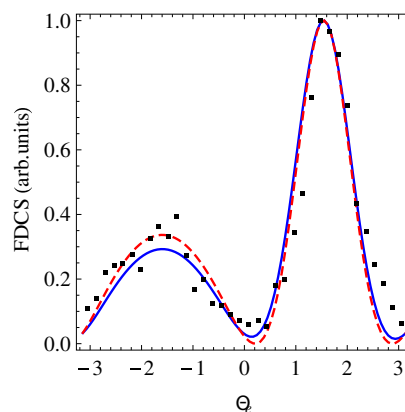


Fig. 1. FDSC in arbitrary units, normalized by the maximum of the distribution for the single ionization of He by 100 MeV/amu C^{6+} ions in the scattering plane ($\phi_e = 0$), for various values of the ejected electron polar angle θ_e , for a momentum transfer of $Q_x = 0.75$ au, $Q_y = 0.02$ au and $Q_z = 0.02$ au, and an ejected electron energy $E_e = 6.5$ eV. The red dashed line shows the FDSC calculated in the traditional coherent form. The blue (solid) line corresponds to the Eq. (4), with $\sigma_x = 0.25$ au and $\sigma_y = 0.5$ au. The black dots correspond to the measurements from [12]. (For interpretation of the references to colour in this figure legend, the reader is referred to the web version of this article.)

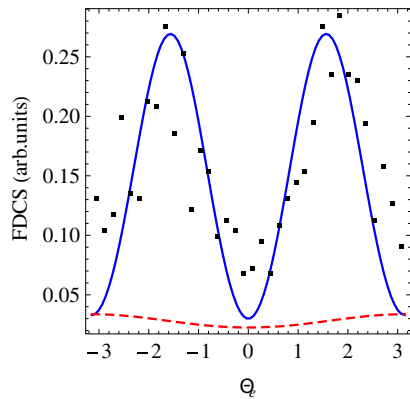


Fig. 2. The same as Fig. 1, for the perpendicular plane: $\phi_e = \pi/2$. The calculations are normalized by the maximum of the curves in the scattering plane.

4.2. p^+ at 1 MeV on He

Now we analyze the data coming from the experiment performed by Gassert et al. [21]. They used protons (p^+) as projectiles at a collision energy of 1 MeV. The final energy of the electron is fixed at $E_e = 6.5$ eV. By fitting Eq. (4) with the experimental data, we found the values: $\sigma_x = 0.054$ au and $\sigma_y = 0.11$ au. In Fig. 3 we can see a very good agreement in the scattering plane ($\phi_e = 0$) between the theoretical calculations and the experimental data, as it was the case for the C^{6+} projectiles.

In Fig. 4, we analyze the azimuthal plane. Here the theoretical results were convoluted with the experimental resolution. To illustrate the good agreement between experiment and both theories the data are presented on a logarithmic scale. As is seen, the incoherent calculation provides a much better description of the two minima near the central maximum than the coherent one.

In [21] the perpendicular plane was not analyzed. However in Fig. 5 we plot the curves coming from the coherent and incoherent calculation of the DDCS (for clarity, they are presented on a logarithmic scale, as in Fig. 4). We can see that there is a disagreement between the coherent and the incoherent calculation, but smaller than the one observed for the case of C^{6+} projectiles, as shown in

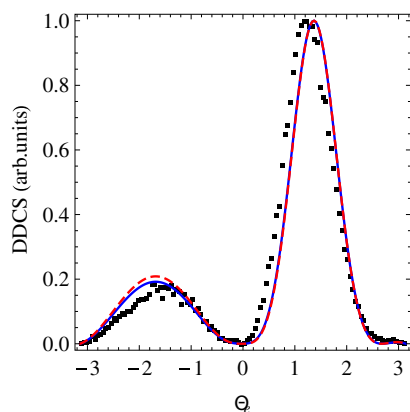


Fig. 3. DDCS in arbitrary units, normalized by the maximum of the distribution for single ionization of He by 1 MeV p^+ in the scattering plane: $\phi_e = 0 \pm 0.18$ (i.e. $\phi_e = 0^\circ \pm 10^\circ$), for various values of the ejected electron polar angle θ_e , at a momentum transfer of $Q_x = 0.75$ au, $Q_y = 0.0$ au $Q_z = 0.02$ au, and an ejected electron energy $E_e = 6.5$ eV. The red dashed line shows the FDCS calculated in the traditional coherent form. The blue (solid) line corresponds to the Eq. 4, with $\sigma_x = 0.054$ au and $\sigma_y = 0.11$ au. The black dots correspond to the measurements from [21]. (For interpretation of the references to colour in this figure legend, the reader is referred to the web version of this article.)

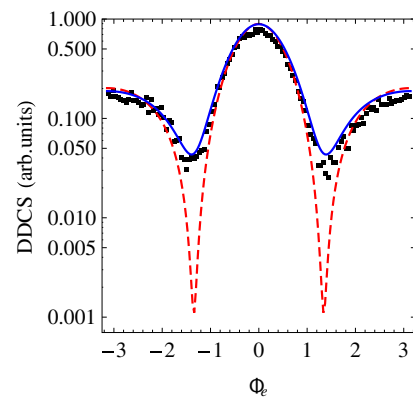


Fig. 4. The same as Fig. 3, for the azimuthal plane: $\theta_e = \pi/2 \pm 0.18$ (i.e. $\theta_e = 90^\circ \pm 10^\circ$).

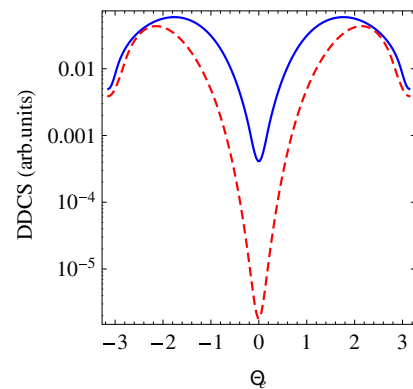


Fig. 5. The same as Fig. 3, for the perpendicular plane: $\phi_e = \pi/2 \pm 0.18$ (i.e. $\phi_e = 90^\circ \pm 10^\circ$).

Fig. 2. The reason of the smaller difference comes from the fact that here the values of σ_x and σ_y are smaller, which means a greater coherence length. Finally, let us point out that the ratio between the two coherent lengths, i.e. $\Delta r_x/\Delta r_y = \sigma_y/\sigma_x \approx 2$ is in a reasonable agreement with the one given in [21], for which they reported $\Delta r_x/\Delta r_y \approx 2.6$.

5. Conclusions

This work confirms the importance of projectile coherence effects and supports the interpretation that discrepancies between experiment and theory reported in the past [12] for 100 MeV/amu C^{6+} on He are due to their influence.

The experimental data [21] for 1 MeV p^+ on He are not inconsistent with that interpretation. It can be seen by the fact that, in the scattering plane, the present model does not predict significant differences between the DDCS calculated both coherent and incoherently. Furthermore, in the azimuthal plane, the incoherent calculation gives a much better agreement with the experiment than the coherent one.

Acknowledgements

We want to thank Dr. Michael Schulz and Dr. Juan Fiol for their advice during the development of this work.

This work was supported by the National Scientific Research Foundation (OTKA, Grant No. K109440), by the project ELI – Extreme Light Infrastructure – phase 2 (CZ.02.1.01/0.0/0.0/15_00

8/0000162) and Universidad Nacional de Cuyo (Grant 06/C480), Argentina.

References

- [1] K.N. Egodapitiya, S. Sharma, A. Hasan, A.C. Laforge, D.H. Madison, R. Moshhammer, M. Schulz, Phys. Rev. Lett. 106 (2011) 153202, <http://dx.doi.org/10.1103/PhysRevLett.106.153202>.
- [2] S. Sharma, A. Hasan, K.N. Egodapitiya, T.P. Arthanayaka, G. Sakhelashvili, M. Schulz, Phys. Rev. A 86 (2012) 022706, <http://dx.doi.org/10.1103/PhysRevA.86.022706>.
- [3] X. Wang, K. Schneider, A. LaForge, A. Kelkar, M. Grieser, R. Moshhammer, J. Ullrich, M. Schulz, D. Fischer, J. Phys. B 45 (2012) 211001, <http://dx.doi.org/10.1088/0953-4075/45/21/211001>.
- [4] J.M. Feagin, L. Hargreaves, Phys. Rev. A 88 (2013) 032705, <http://dx.doi.org/10.1103/PhysRevA.88.032705>.
- [5] K. Schneider, M. Schulz, X. Wang, A. Kelkar, M. Grieser, C. Krantz, J. Ullrich, R. Moshhammer, D. Fischer, Phys. Rev. Lett. 110 (2013) 113201, <http://dx.doi.org/10.1103/PhysRevLett.110.113201>.
- [6] S. Sharma, T.P. Arthanayaka, A. Hasan, B.R. Lamichhane, J. Remolina, A. Smith, M. Schulz, Phys. Rev. A 90 (2014) 052710, <http://dx.doi.org/10.1103/PhysRevA.90.052710>.
- [7] F. Járjai-Szabó, L. Nagy, Eur. Phys. J. D 69 (2015) 4, <http://dx.doi.org/10.1140/epjd/e2014-50640-2>.
- [8] T.P. Arthanayaka, S. Sharma, B.R. Lamichhane, A. Hasan, J. Remolina, S. Gurung, L. Sarkadi, M. Schulz, J. Phys. B 48 (2015) 175204, <http://dx.doi.org/10.1088/0953-4075/48/17/175204>.
- [9] T. Arthanayaka, B.R. Lamichhane, A. Hasan, S. Gurung, J. Remolina, S. Borbély, F. Járjai-Szabó, L. Nagy, M. Schulz, J. Phys. B 49 (13) (2016) 13LT02, <http://dx.doi.org/10.1088/0953-4075/49/13/13LT02>.
- [10] L. Sarkadi, I. Fabre, F. Navarrete, R.O. Barrachina, Phys. Rev. A 93 (2016) 032702, <http://dx.doi.org/10.1103/PhysRevA.93.032702>.
- [11] J.R. Taylor, Scattering Theory: The Quantum Theory on Nonrelativistic Collisions, John Wiley & Sons Inc, Hoboken, New Jersey, 1972.
- [12] M. Schulz, R. Moshhammer, D. Fischer, H. Kollmus, D.H. Madison, S. Jones, J. Ullrich, Nature 422 (2003) 48, <http://dx.doi.org/10.1038/nature01415>.
- [13] I. Fabre, Master's Thesis, Instituto Balseiro-Universidad Nacional de Cuyo, 2015.
- [14] I. Fabre, F. Navarrete, L. Sarkadi, R.O. Barrachina, J. Phys. Conf. Ser. 635 (2015) 012001, <http://dx.doi.org/10.1088/1742-6596/635/4/042003>.
- [15] D.V. Karlovets, G.L. Kotkin, V.G. Serbo, Phys. Rev. A 92 (2015) 052703, <http://dx.doi.org/10.1103/PhysRevA.92.052703>.
- [16] J. Fiol, S. Otranto, R.E. Olson, J. Phys. Conf. Ser. 88 (2007) 012014, <http://dx.doi.org/10.1088/1742-6596/88/1/012014>.
- [17] J. Fiol, S. Otranto, R.E. Olson, J. Phys. Conf. Ser. 58 (2007) 161, <http://dx.doi.org/10.1088/1742-6596/58/1/031>.
- [18] J. Fiol, S. Otranto, R.E. Olson, J. Phys. B 39 (2006) L285, <http://dx.doi.org/10.1088/0953-4075/39/14/L02>.
- [19] K.A. Kouzakov, S.A. Zaytsev, Y. Popov, M. Takahashi, Phys. Rev. A 86 (2012) 032710, <http://dx.doi.org/10.1103/PhysRevA.86.032710>.
- [20] J. Colgan, M.S. Pindzola, F. Robicheaux, M.F. Ciappina, J. Phys. B 44 (2011) 175205, <http://dx.doi.org/10.1088/0953-4075/44/17/175205>.
- [21] H. Gassert, O. Chuluunbaatar, M. Waitz, F. Trinter, H.-K. Kim, T. Bauer, A. Laucke, C. Müller, J. Voigtsberger, M. Weller, J. Rist, M. Pitzer, S. Zeller, T. Jahnke, L.P.H. Schmidt, J.B. Williams, S.A. Zaytsev, A.A. Bulychev, K.A. Kouzakov, H. Schmidt-Böcking, R. Dörner, Y.V. Popov, M.S. Schöffler, Phys. Rev. Lett. 116 (2016) 073201, <http://dx.doi.org/10.1103/PhysRevLett.116.073201>.